

Phase Separation Models for Cuprate Stripe Arrays

R.S. Markiewicz and C. Kusko

Physics Department and Barnett Institute, Northeastern U., Boston MA 02115

An electronic phase separation model provides a natural explanation for a large variety of experimental results in the cuprates, including evidence for both stripes and larger domains, and a termination of the phase separation in the slightly overdoped regime, when the average hole density equals that on the charged stripes. Several models are presented for charged stripes, showing how density waves, superconductivity, and strong correlations compete with quantum size effects (QSEs) in narrow stripes. The energy bands associated with the charged stripes develop in the middle of the Mott gap, and the splitting of these bands can be understood by considering the QSE on a single ladder.

I. INTRODUCTION

Possible electronic phase separation (EPS) in the cuprates has usually been found in terms of stripe phases. Thus, neutron diffraction measurements find evidence for fluctuating stripe order in $\text{La}_{2-x}\text{Sr}_x\text{CuO}_4$ (LSCO) associated with incommensurate inelastic neutron scattering¹, which can be transformed into long range charged stripe order² by co-doping with Nd or Eu. Similar incommensurate peaks are found in other cuprates, and long range charge ordered states are also found³ in strongly underdoped samples of $\text{YBa}_2\text{Cu}_3\text{O}_{7-\delta}$ (YBCO), with stripes parallel to the chains, while at higher doping short range stripe order is found at virtually all temperatures up to the pseudogap T^* . However, EPS can also manifest itself in the form of *larger domains*, particularly if the dopant ions are somewhat mobile and can follow the hole motion. These domains, long known in $\text{La}_2\text{CuO}_{4+\delta}$ may recently have been found in scanning tunneling microscope (STM)⁴ and microwave⁵ studies of $\text{Bi}_2\text{Sr}_2\text{CaCu}_2\text{O}_{8+\delta}$ (Bi2212).

Stripes are typically interpreted either in terms of charged domain walls in antiferromagnets or of restricted EPS. While the models are virtually indistinguishable in the underdoped regime, they diverge as doping increases. A phase separation model implies the existence of a uniform end phase: at some doping antiferromagnetic (AFM) stripes must disappear, leaving a uniform state similar to that found on the charged stripes. For slightly lower doping the AFM stripes form a minority – a situation not possible in a domain wall picture. (A note of caution: more recent domain wall models find a lower doping on the charged stripes, and as the doping decreases, the distinction between the two models gradually blurs.) Evidence for the termination of the AFM stripes at a fixed doping⁶ and recent observations of larger domain structures⁴ taken together provide ex-

tremely strong support for a phase separation scenario.

At this point it is essential to better characterize the nature of the stripes, in particular the charged stripes, and to understand how their properties affect physical phenomena, in particular photoemission spectra.^{7–11} While fluctuations^{7,8} play an important role in the real cuprates, we have constructed ordered stripe arrays, for which detailed tight-binding calculations are possible⁹. Such calculations can aid in elucidating the structure of the charged stripes, both for wide stripes – what stabilizes the preferred hole density – and for narrow stripes – how do quantum size effects (QSE) modify properties of the stripes. The present paper provides an extended analysis of these issues; some of these results were summarized recently¹².

The paper is organized as follows. Section II enumerates key issues which must be addressed in any EPS model of stripes, including determination of the hole density on charged stripes. It is found that the model can simultaneously account for a large number of experimental results. The charged stripes are probably stabilized by some competing order, either magnetic or paramagnetic (including charge density waves). Section III shows that magnetic charged stripes can arise in a mean field Hubbard model, and can be either ferromagnetic or a linear antiferromagnetic (LAF) phase similar to the White-Scalapino stripes¹³. Calculations on stripe arrays find that the charged stripes lead to midgap states near the Fermi level; Section IV shows how these data can be interpreted in terms of quantum size effect (QSE) on single stripes. Section V presents the results of single stripe calculations: competing charge density wave (CDW) and superconducting orders can exist on paramagnetic stripes, but they are strongly modified by the QSE. On LAF stripes, d-wave superconductivity and an unusual form of CDW are both found to persist down to the narrowest (2 cells wide) stripes. Section VI includes results on stripe arrays: the LAF stripes produce photoemission constant-energy maps in significantly better agreement with experiment. In the Discussion, Section VII, we summarize additional recent evidence which favors a phase separation model – in particular, evidence that AFM stripes terminate slightly beyond optimal doping, where superconducting properties remain strong, and that a second regime of phase separation exists above optimal doping – and we show that experiments are consistent with our prediction that the superconducting gap grows in the underdoped regime. Conclusions are given in Section VIII.

II. KEY ISSUES FOR AN EPS MODEL OF STRIPES

A phase separation model of stripes is characterized by the two well-defined stable end phases between which phase separation takes place. The insulating stripes are generally understood to be antiferromagnetic (AFM) – essentially the same as the Mott insulator found in undoped cuprates. The hole-doped stripes are assumed to have a finite doping, x_0 . This simple idea has three experimentally verifiable characteristic features: (i) *the stripe phase must terminate* when $x = x_0$; (ii) there will be a *crossover* at a lower doping, $x_{cr} \sim x_0/2$ from magnetic-dominated ($x < x_{cr}$) to charge-dominated ($x > x_{cr}$) stripe arrays; (iii) some *interaction* on the charged stripes stabilizes the end phase at x_0 . Here we discuss current evidence for (a) the doping on the charged stripes, (b) evidence for a crossover, and (c) the nature of the dominant interaction stabilizing the charged stripes. In addition, we ask what constraints the Yamada plot puts on the model, and how a model based on EPS compares to a domain wall model.

A. Hole Doping on Charged Stripes

Recent evidence suggests that the stripes and pseudogap terminate at the same doping x_0 while superconductivity persists to higher doping⁶. However, the proper choice of x_0 requires some discussion. The neutron diffraction measurements of Tranquada² and Yamada¹ have established that charged stripes in $\text{La}_{2-x}\text{Sr}_x\text{CuO}_4$ (LSCO) have an invariant topology over the doping range $0.06 \leq x \leq 0.125$, acting as antiphase boundaries (APBs) for the AFM stripes and having a net doping of 0.5 holes per stripe. However, there are two models for how this charge is distributed: either in one row with average hole density 0.5 hole per copper site or in two rows with 0.25 hole per copper. These two alternatives are often somewhat simplistically referred to as site order vs bond order. The strongest evidence distinguishing between the alternatives comes from x-ray data on the charge order¹⁴ at $x=1/8$: non-observation of diffraction harmonics suggests a sinusoidal distribution of charge. For a 4-Cu repeat distance, two insulating and two charged rows would be exactly sinusoidal, whereas one charged and three insulating rows should have significant harmonic content. A similar conclusion was reached by μSR line-shape analysis¹⁵. However, the charge ordering peaks are weak, and it remains possible that fluctuations or disorder could wash out the harmonics.

Direct evidence for the density on the charged stripes is found from low temperature NQR measurements¹⁶, which find values $x_0 \sim 0.18 - 0.19$. While this is close to the lower value, the small difference can also be understood: this is a *local* measurement, and it is expected that some holes will be pushed off onto the magnetic stripes.

Indirect evidence favoring the lower hole density includes the fact that it is easier to understand the properties of AFM stripes in terms of even-leg ladders (e.g., the AFM stripes would be two coppers wide at $x=1/8$)¹⁷, and that the stripe phase appears to terminate when the average doping approaches $x=0.25$ (Section VII.A.1). The lower doping is also more consistent with the tJ model simulations of White and Scalapino¹³.

Tallon¹⁸ finds an optimal doping at $x_{opt} = 0.16$ for all cuprates, with respect to which the stripes terminate at a doping $x = 0.19$. However, it is hard to reconcile a common optimal doping with muon spin resonance data¹⁹, which find T_c is optimized at very different values of n_s/m (n_s is the pair density, which seems to scale with carrier concentration²⁰, and m effective mass) for LSCO and YBCO. We assume instead that x_{opt} scales with n/m , so if $x_{opt} = 0.16$ for LSCO, it is 0.21 for YBCO, in good agreement with several estimates²¹. This also resolves a problem with the thermopower. While the thermopower appears to be universal for most cuprates, and the best means of estimating the doping is from the room temperature thermopower, LSCO is anomalous in that ‘overdoped’ samples still have high thermopower²². If the doping for YBCO is rescaled as above, however, the thermopower data of LSCO fall on the universal curve. Hence, the anomaly for LSCO is not in the thermopower, but in a too low value of T_c , which is accompanied by a too low value of x_{opt} . It is likely that these features are associated with a competing LTT phase, which is most prominent in LSCO, and which also leads to the most nearly static stripe correlations.

Taking $x_{opt}=0.21$ for YBCO gives $x_0 = 19/16 \times 0.21 = 0.25$, which we believe holds for *all cuprates*, including LSCO, Section VII.A.1. This would lead to very wide charged stripes near optimal doping: the width of the charged stripes N satisfies $N/(N+2) = 16/19$, or $N = 32/3 \sim 10$ Cu wide. Hence, models of isolated quasi-one-dimensional charged stripes are likely to be valid only in the far underdoped regime, while for the good superconductors a better model would be a metal with intrinsic weak links²³.

B. Crossover at 1/8 Doping

For $x_0 \sim 1/4$, the crossover $x_{cr} = x_0/2$ can be identified with the 1/8 anomaly, where both charged and AFM stripes have their minimal width (2 Cu atoms). There is considerable evidence that the doping 1/8, in addition to its special stability, acts as a crossover in the properties of the stripes. Thus, Uchida, et al.²⁴, studying the Hall coefficient R_H , find a crossover from one-dimensional behavior ($R_H \rightarrow 0$ as $T \rightarrow 0$) for $x < x_{cr} = 1/8$ to two-dimensional behavior (coupled charged stripes) for $x > x_{cr}$. In YBCO, the spin gap grows slowly with doping for $x < x_{cr}$, then more rapidly for $x > x_{cr}$; this behavior can be understood in terms of coupled spin ladders, as the

coupling changes with the width of the charged stripes⁹. In Eu substituted LSCO²⁵, the Meissner fraction is negligibly small for $x < x_{cr}$, then grows roughly linearly with doping until $x \simeq 0.18$, staying large up to at least $x = 0.22$. Finally, the two-magnon Raman peak in LSCO has a splitting at low temperatures which has been associated with stripes²⁶, on analogy with similar observations in $\text{La}_{2-x}\text{Sr}_x\text{NiO}_4$ (LSNO)²⁷. For $x < x_{cr}$ the ratio of the two peak frequencies is constant and consistent with a simple stripe model; for $x > x_{cr}$ the lower frequency starts decreasing with doping. Moreover, the higher frequency loses intensity with doping; near $x = 0.26$, the *intensity* of one mode approximately disappears, while the *frequency* of the other mode extrapolates to zero.

C. Constraints from the Yamada Plot

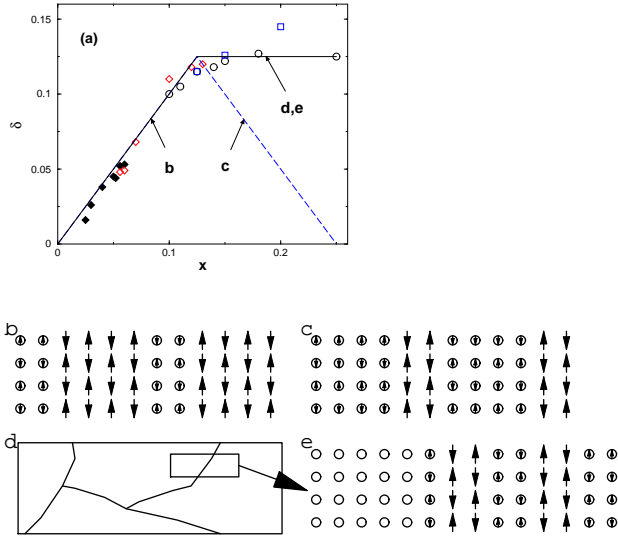


FIG. 1. (a) Yamada plot of incommensurability δ vs doping x for LSCO. Open squares = elastic neutron scattering in Nd substituted samples²; others = inelastic neutron scattering for vertical stripes (open circles¹ or diamonds²⁸) or diagonal stripes (filled diamonds²⁸). Dashed (solid) line = prediction of EPS model without (with) commensurability effect at $1/8$ doping. (b,c) = Stripe phase model without commensurability effect, at $x = 1/12$ (b) and $1/6$ (c). For this figure, the charged stripes are assumed to have linear antiferromagnetic order (Section III). (d,e) = domains associated with commensurability pinning of $1/8$ doped phase; (e) = blowup of (d).

The Yamada^{1,2,28} plot, Fig. 1a, provides a severe constraint on any model of stripes: in LSCO the incommensurability δ is found to grow linearly with doping for $x < x_{cr}$ but to saturate for $x > x_{cr}$. Furthermore, the saturation value is just the incommensurability expected for $x = 1/8$ -doped stripes, $\delta_{sat} = x_{cr}$. A similar saturation has been reported in YBCO, but different groups find different values for δ_{sat} : $\sim 1/6$ [29] or $\sim 1/10$ [30].

If one of these values proves correct, it would suggest some nonuniversality in x_0 , perhaps associated with bilayer splitting. In the domain wall model, the saturation is interpreted as evidence that the stripes stop changing in width, and additional holes leak into the antiferromagnetic background, washing out the stripes.

For $x \leq 1/8$, the EPS model agrees with the Yamada plot, Fig. 1b: increase in doping causes the AFM stripes to narrow, with no changes in the charged stripes. Note that, for concreteness we have assumed that the charged stripes have LAF order (Section III); these stripes naturally act as antiphase boundaries (APBs), consistent with the neutron evidence. However, the naive prediction of the EPS model is in disagreement with the Yamada plot for $x > 1/8$, Fig. 1c: as the charge stripes get wider, the incommensurability should decrease, while the neutron peaks may broaden if the wider charge stripes do not act as APBs. This behavior is not observed. However, the model can be simply modified to explain the observed saturation, Fig. 1d,e. This would be a commensurability effect, with part of the sample pinned at $1/8$ doping while the rest forms a different phase (e.g., at $1/4$ doping) where no stripes are present. Such behavior is well known in nickelates, where coexistence of $1/3$ and $1/2$ stripes is common.

Evidence for such commensurability effects can be found by comparing¹² the chemical potential μ in LSCO³¹ and LSNO³². In both materials, μ is approximately independent of doping between half filling ($x = 0$) and x_{cr} , with $x_{cr} = 0.125$ in LSCO, $1/3$ in LSNO, which has long-range charge order. Remarkably, the simple prediction of a macroscopic phase separation model (μ constant throughout the phase separation regime) is violated in LSNO: μ is *not* constant for $1/3 < x < 1/2$, although the stripe phase persists over the full doping range. This is presumably a commensurability effect, reflecting the coexistence of $1/3$ and $1/2$ stripe phases for intermediate dopings. The same doping dependence of μ is found in LSCO: constant for $x < 1/8$, variable for $x > 1/8$. Indeed, the LSNO data can be scaled to that of the cuprates, giving a common doping dependence $\mu(x/x_c)$ in both compounds¹².

D. Domain Phase

Recently local charged domains have been directly visualized by STM studies in Bi2212⁴ with gaps ranging from slightly overdoped to strongly underdoped. Such behavior is extremely difficult to explain in the domain wall picture, but is easy to understand in terms of EPS, and indeed is consistent with the commensurability effects discussed above. The gap distribution is found to be broad rather than bimodal, but that is expected since EPS is very sensitive to charged impurities, and the local gap will correlate with the local density of dopant, presumably interstitial oxygen in Bi2212. This sensitivity

to impurities leads to the question of which came first: is a preexisting EPS sensitive to local impurities, or does oxygen clustering³³ provide the driving mechanism for domain formation? Since the electronic inhomogeneity seems characteristic of most cuprates while there is considerable variety in the doping counterions, the simpler interpretation would appear to be that the EPS is primary. Thus, in $\text{La}_2\text{CuO}_{4+\delta}$ (LCO), the interstitial oxygens are highly mobile, allowing the domains to grow to macroscopic size. Similar clusters form in YBCO (here associated with chain oxygens), but can be suppressed in fully oxygenated samples by quenching³⁴. On the other hand, well formed stripes appear when the doping counterions are least mobile, in LSCO.

The domains in Bi2212 would seem to be consistent, but a number of questions remain about the role of annealing. While these domains are regularly found in STM studies when the samples are cleaved at low-temperature, they can be annealed out at high temperatures³⁵. This could be caused by a ‘melting’ of the EPS, as is found in LCO near room temperature³⁶, and can be tested by careful annealing studies. Alternatively, it may be a question of pinning the EPS. Certainly, it is known that a weak domain disorder is necessary to pin vortices, to observe the vortex lattice via STM.³⁴ Also, the role of the interstitial oxygen in the superlattice modulations in Bi2212 needs to be better understood. The strength of this modulation suggests that it is associated with an ordering of the interstitial oxygen, but this should lead to a strong correlation between the domains and the superlattice, which seems not to be the case. Further evidence for electronic inhomogeneity comes from microwave measurements: anomalies in Bi2212 have been interpreted in terms of similar electronic domains⁵, suggesting that they are representative of the bulk, while measurements on other cuprates³⁷ find similar anomalous behavior which was interpreted in terms of pinned CDW’s, possibly stripe related. A domain picture would also explain the persistence of nodal quasiparticles in the underdoped regime, at least down to $1/8$ doping³⁸.

E. Comparison of Domain Wall Stripes and EPS Stripes

Table I summarizes the discussion of the previous subsections, and compares the predictions of EPS models

Table I: Comparison of Stripe Models

Model	$\frac{1}{8} < x < \frac{1}{4}$	APB?	saturation at $x > \frac{1}{8}$?	domains?	crossover at $x = \frac{1}{8}$?	termination at $x \sim \frac{1}{4}$?
Domain wall	fixed pattern holes spread out	✓	✓	×	?×	?×
EPS (simple)	charge stripes grow in width	~	×	×	✓	✓
EPS (commensurate pinning)	domain phase: $x = \frac{1}{8}$: stripes $x = \frac{1}{4}$: uniform	~	✓	✓	✓	✓

with domain wall models of stripes. Domain wall models arose in early unrestricted Hartree-Fock (UHF) calculations^{59–61} for the doped tJ model, as heterogeneous ground states in which the holes are confined to domain walls between AFM domains which act as APBs. These domain walls are not driven by phase separation⁶²; the phase is realized as a long-period modulated AFM, with holes doping the rows of spins where the moment changes sign⁴⁰. When $t' = 0$, there is one hole per row, a large hole doping which is inconsistent both with experiments on stripes in the cuprates, and with density matrix renormalization group (DMRG) calculations¹³. More recent calculations reduce the doping, in ways that bring the model close to the phase separation picture: (1) assuming CDW order along the charged stripes³⁹ lowers x_0 to 0.5, while (2) letting $t' < 0$ results in $x_0 \sim 0.2$.⁴⁰ Since the CDW order (case 1) lowers the free energy of the charged stripes, it should be possible to dope the system all the way to a pure CDW at $x = 0.5$. In case 2, it is not explained why a low density appears; a good possibility is that this doping corresponds to the Van Hove singularity (VHS), as in the phase separated stripes. (This could be checked by varying t' and calculating $x_0(t')$.) If such low-density domain walls do exist, the striped phase must somehow terminate when the average doping approached 0.2, but how this happens is not explained. However, this calculation⁴⁰ is not fully UHF, being restricted to periodic arrays, and UHF calculations⁴¹ find instead ferromagnetic charged stripes which can be understood within a phase separation model (see below).

Since the stability of these $t' \neq 0$ domain wall stripes is unclear, in Table I a comparison is made with the earlier, higher-hole-density domain wall models. For such high doping, stripe termination at $x = 1/4$, or a major crossover near $1/8$, are both difficult to interpret. Stripes as APBs are more natural in domain wall models, but we shall show that they can also arise in EPS models. Note that the distinction between the models may be becoming moot, since in the domain wall models there is now a search for a ‘hidden’ order parameter⁴², and it is common for secondary order parameters to be expressed predominantly on domain walls of the primary order⁴³.

In conclusion, assumption of a charged stripe doping $x_0 \simeq 0.25$ reconciles the neutron diffraction data, evidence for a termination of the stripe phase near x_0 , and the $1/8$ anomaly as a crossover effect near $x_0/2$, while

commensurability effects can explain the saturation in the Yamada plot and the STM observation of charge domains. Further supportive evidence will be presented in Section VII.A. In the remainder of this paper, we will assume that $x_0 = 0.25$.

F. What Stabilizes Charged Stripes?

In any phase separation model, a key issue is understanding the nature of the charged stripes. Indeed, since superconductivity seems to arise predominantly on these stripes, such understanding is likely to play an important role in elucidating the origin of the high superconducting transition temperatures. For the stripe phase to exist, the doping x_0 must be particularly *stable*. This can arise via an electronic *instability*, which opens up a gap over much of the Fermi surface, making the electronic phase nearly incompressible. This ‘Stability from Instability’ is a fairly general feature, underlying, e.g., Hume-Rothery alloys⁴⁴. [This is a modification of an argument due to Anderson⁴⁵.] Here, we explore a number of candidates for the predominant electronic instability.

In a related paper⁶⁶, we will provide strong evidence that this ‘hidden order’ is a form of CDW, which could include the flux phase. However, here we will explore a wider variety of possibilities. One issue is that in the low doping limit the charge stripes act as APBs for the AFM stripes. Such an effect arises naturally if the charged stripes have some residual magnetic interaction, and we will explore this possibility. However, in nickelates charged stripes coupled to a CDW are found to act as APBs⁴⁶. The large Hubbard on-site repulsion U plays an important role. Strong correlation effects lead to two classes of charged stripe phases: either the constraint against double occupancy leads to magnetic order (magnetic charged stripes) or kinetic energy dominates, leading to a magnetically disordered phase (paramagnetic charged stripes), with correlations leading to reduced hopping, as in tJ⁴⁷ and slave boson⁴⁸ models. Section III will provide examples of both classes, denoted as Class B and Class A stripes, respectively. Class A stripes could be simply correlated metals (as in tJ or slave boson calculations) or could have additional, e.g., CDW, order. A crossover from magnetic to correlated paramagnetic groundstate arises as a function of doping in models of itinerant ferromagnets⁴⁹.

For completeness, Class C stripes are defined as those arising not from phase separation but from long-range modulated AFM order (domain wall stripes). Such stripes have been described in detail⁴⁰, and will not be further considered here.

In the next Section, we show that Class B (magnetic) charge stripes can arise in a mean-field Hubbard model⁵⁰, with the charged stripes displaying either ferromagnetic (FM) or linear antiferromagnetic (LAF) (ordering vector $(\pi, 0)$) order. The LAF stripes are very similar to White-

Scalapino stripes¹³. The FM phase is stabilized by VHS nesting. This FM phase may be present in ruthenates⁵¹, but is unlikely to be relevant for the cuprates (for one thing, the FM stripes are likely to be diagonal, and do not form APBs⁴¹, contrary to experiment). We have suggested that other VHS-stabilized phases are more likely⁵² (see also Ref. 53), and here we explore the properties of a Class A CDW phase⁴⁸. At a doping $x \sim 0.25$, the effects of correlations are relatively weak, renormalizing the bandwidth by a factor of ~ 2 . Thus for the present calculations on paramagnetic stripes, it will be assumed that renormalized parameters are used, and other effects of strong correlations will be neglected.

While LAF stripes are most stable when $t' = 0$, we explore the possibility that they can be stabilized even when $t' \neq 0$ by on-stripe CDW or superconducting order. Ordinarily, the CDW phase is believed to *compete* with strong correlation effects, but we find (Section V.B) that an unusual form of CDW phase can *coexist* with LAF order: the charge density varies between zero and one (not two) holes per atom.

G. Notation on Stripes

In a stripe array, the alternating stripes are associated with the two stable thermodynamic phases. Here, we summarize the different ways these stripes are denoted in this paper. The stripe with lower hole doping is variously referred to as ‘insulating’ or ‘antiferromagnetic’ (AFM). (These are also known as magnetic stripes, since the charged stripes have considerably weaker magnetic order, but we will avoid that notation here.) The stripe with higher hole doping is generically referred to as ‘charged’ or ‘hole-doped’. At low temperatures, these stripes are also ‘superconducting’, but at high temperatures, they are stabilized by some ‘hidden order’, and one purpose of this paper is to explore a number of possible orders. The orders fall into two groups: ‘magnetic charged’ (Class B) stripes could have FM or LAF order (the latter are White-Scalapino-like stripes), while ‘paramagnetic’ (Class A) stripes could have CDW or flux-phase order.

III. PHASE SEPARATION IN A MEAN-FIELD HUBBARD MODEL

Strong coupling models would seem to be natural for producing phase separated or striped ground states. Any magnetic ordering avoids double occupancy, while changing from one form of magnetic order to another, via, e.g., doping, requires highly collective spin rotations, as competing orders are orthogonal. While superexchange leads to antiferromagnetic (AFM) insulators at half filling, doping tends to favor textures with parallel spins (e.g., ferromagnetic (FM)) to maximize hole hopping. Such

ferron phases were introduced long before high T_c ⁵⁴, but it remains controversial whether such states are ground states of the Hubbard model⁵⁵. While the tJ model does have phase separation for large J/t , it is unclear whether such phases extend to the values $J/t \sim 0.3$ expected for the cuprates^{13,56–58}.

We have found phase separated solutions of the Hubbard model at mean-field level⁵⁰. While these solutions are metastable in UHF calculations, they closely resemble the WS stripes, and provide an interesting example of phase-separation mediated stripe phases. We find a well defined surface tension for wide, isolated stripes, which decreases and changes sign as the stripes become narrower. When the surface tension becomes negative, the stripes no longer remain straight, and spontaneously meandering solutions are found.

These solutions are found by considering only low-order commensurate phases, with wave vector $q_x, q_y \sim 0$ or $Q_i = \pi/a$ only. The bare dispersion is

$$\epsilon_k = -2t(c_x + c_y) - 4t'c_x c_y, \quad (1)$$

with $c_i = \cos k_i a$. The Hubbard interaction $U \sum_i (n_{i\uparrow} - 1/2)(n_{i\downarrow} - 1/2)$ leads to magnetic order with a mean-field magnetization m_q at wave vector \vec{q} , and the quasiparticle dispersion becomes

$$E_{\pm} = \epsilon_{\pm} \pm E_0, \quad (2)$$

where

$$E_0 = \sqrt{\epsilon_{-}^2 + U^2 m_q^2} \quad (3)$$

and

$$\epsilon_{\pm} = \frac{1}{2}(\epsilon_k \pm \epsilon_{k+q}) \quad (4)$$

For the cuprates, we expect⁹ $t \simeq 325\text{meV}$, $U/t \simeq 6$ and $t'/t \simeq -0.276$. The magnetization is found self-consistently from

$$m_q = \sum_k (f(E_-) - f(E_+)) \frac{U m_q}{2E_0}, \quad (5)$$

with Fermi function $f(E) = 1/(1 + e^{(E-E_F)/k_B T})$. The resulting free energy is

$$F = E_q - TS + U(m_q^2 + \frac{x^2}{4}), \quad (6)$$

with

$$E_q = \sum_{k,i=\pm} E_i f(E_i), \quad (7)$$

$$S = k_B \sum_{k,i=\pm} (f(E_i) \ln(f(E_i)) + (1 - f(E_i)) \ln(1 - f(E_i))). \quad (8)$$

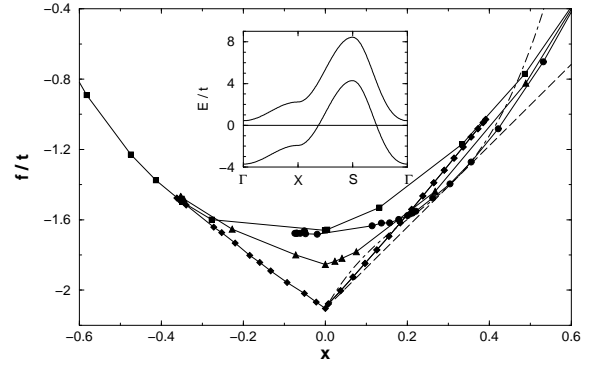


FIG. 2. Free energy vs. doping for several magnetic phases of the Hubbard model assuming $U = 6.03t$, and $t' = -0.276t$. Diamonds = AFM, triangles = LAF, circles = FM, and squares = PM phase. Dashed lines = tangent construction; dot-dashed line = Eq. 9. Inset: Dispersion of FM phase at $x = 0.31$; Brillouin zone points $\Gamma = (0, 0)$, $X = (\pi, 0)$, $S = (\pi, \pi)$.

The competing phases include AFM for $\vec{q} = \vec{Q} \equiv (\pi, \pi)$, FM with $\vec{q} = (0, 0)$, and a linear antiferromagnet (LAF) with $\vec{q} = (\pi, 0)$. When the LAF stripes are two cells wide, this LAF phase closely resembles the White-Scalapino stripes, Fig. 1e. The AFM state has lowest free energy at half filling, but (for $t' = 0$) is unstable for finite hole doping. For $t' = 0$, there is phase separation between the AFM and LAF phases, while for finite t' the phase separation is between AFM and FM phases, Fig. 2. (When electron-phonon coupling is included, it is found that the FM phase is unstable with respect to a CDW phase⁶⁶.)

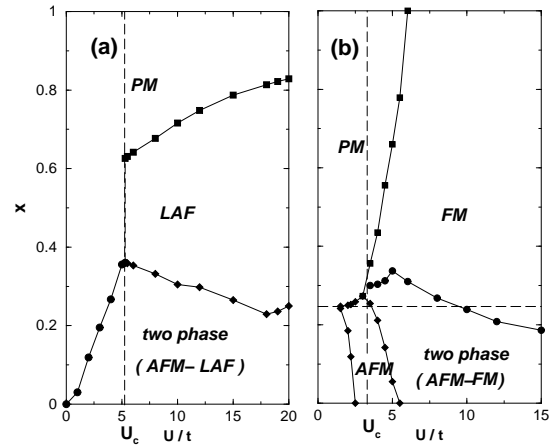


FIG. 3. Phase diagrams, $x(U)$ for the Hubbard model, with $t' = 0$ (a) or $t' = -0.276t$ (b). (Dashed line in (b) = doping of VHS.)

The LAF stripes for $t' = 0$ are discussed in Ref. 50. For $t' \neq 0$ electron-hole symmetry is absent; for hole doping $x > 0$, there is phase separation to a FM phase, con-

sistent with recent simulations by Vozmediano, et al.⁴¹, who find a uniform FM phase at $x = 0.15$ for $U = 8t$, $t' = 0.3t$. However, *on the electron-doped side a uniform AFM phase is stable over a large doping range*, suggestive of the asymmetry found in the cuprates. The dot-dashed curve shows that in the phase separation regime, the low energy physics can be approximated by the form of free energy assumed in Ref. 9,

$$f(x) = f_0 x \left(1 - \frac{x}{x_0}\right)^2, \quad (9)$$

(neglecting a term linear in x) with x_0 the hole doping of the uniform charged phase. The FM phase is stabilized by VHS nesting, inset to Fig. 2, as found previously⁵¹. The tangent construction tends to select the FM phase at dopings somewhat away from optimal nesting (Fermi energy above midgap). Both regimes of phase separation seem to be driven by hole delocalization: one-dimensional (along the LAF rows) when $t' = 0$, two-dimensional for finite t' .

The resulting phase diagrams x vs U , Fig. 3, are strikingly different. For $t' = 0$, Fig. 3a, the phase separation is between the AFM and paramagnetic (LAF) phase for $U < U_c = 5.3t$ ($U > U_c$), while for finite t' , Fig. 3b, there is generally a VHS-stabilized FM phase. For small U and $t' \neq 0$, there is a regime where simple spin-density wave theory works and a uniform AFM phase is stable, but when $t' = 0$ phase separation persists for all finite U . Note that U_c marks a crossover between Class A (paramagnetic) and Class B (magnetic) charged stripes. The value U_c is close to the $U = 6.03t$ expected in the cuprates, although for finite t' U_c decreases, $U_c \sim 3t$ for $t' = -0.276t$, and the range of U for which paramagnetic stripes are stable becomes very small. While these stripes are metastable in UHF calculations, we will show below that the stability of phase separating stripes can be enhanced by *additional interactions* beyond the pure Hubbard model.

IV. ISOLATED STRIPES VS. ARRAYS

In ordered stripe arrays it is found⁹ that the AFM stripes have a Mott-Hubbard gap, and the features near the Fermi level are associated with the charged stripes. This charge stripe dispersion shows a series of quasi-one-dimensional features which qualitatively resemble the bands of an isolated stripe produced by QSE. In this Section, we make a quantitative comparison with isolated stripes, and explore the mechanism of QSE-induced Van Hove splitting.

For a single stripe N Cu atoms wide, the dispersion is still given by Eq. 1, but the allowed k_x values are quantized, with $k_x = k_m \equiv m\pi/(N + 1)$, $m = 1, 2, \dots, N$. These are in fact the usual quantized Bloch bands, but for large N the quantization is not noticeable. For small N ,

the dispersion appears as a series of N overlapping one-dimensional (1d) dispersions. Equation 1 can be rewritten as N 1d dispersions

$$\epsilon_{m,k_y} = -2tc_m - 2(t + 2t'c_m)c_y, \quad (10)$$

These are the QSE, with corresponding density of states (dos) shown in Fig. 4. Notice that for $N = 100$, the VHS is readily apparent in the dispersion. Even down to $N = 2$, the VHS is clearly defined (albeit only within a finite interval) as the *locus of energies where all subbands overlap*. In fact, *the QSE opens a gap at the VHS*, effectively lowering the kinetic energy of the electrons just like a conventional (e.g., CDW) gap. The VHS splitting can be found from Eq. 10:

$$\Delta E_{VHS} = \epsilon_1^{max} - \epsilon_N^{min} = 4t(1 - c_1). \quad (11)$$

This splitting has two consequences: first, the VHS splitting enhances the stabilization of the striped phase; but second, the QSE gap competes with other gaps, such as CDW's and superconductivity. However, while the QSE splits the VHS peak, substantial dos remains ungapped, so additional instabilities remain possible. This competition will be discussed further in the next Section.

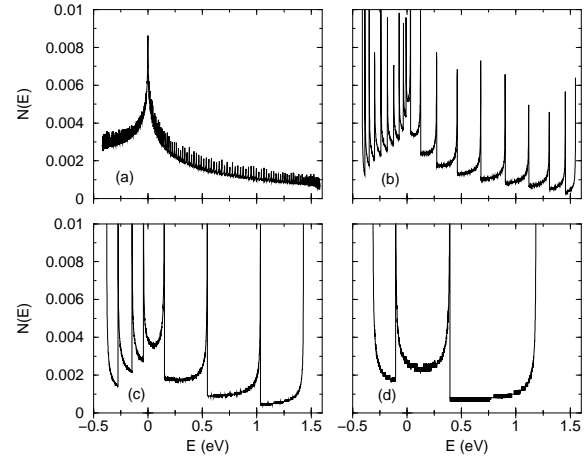


FIG. 4. Density of states for a single stripe of width $N = 100$ (a), 10 (b), 4 (c), or 2 (d) atoms. Based on Eq. 1 with $t'/t = -0.276$.

It should be noted that this is the first direct demonstration that the VHS can be defined on a stripe only two atoms wide. The definition is quite analogous to the standard definition in two dimensions: the point at which the bands cross over from electron-like to hole-like.

Figure 5 compares the gaps of a single stripe with those found in the ordered stripe array⁹; the array is labelled (m, n) when the magnetic stripes are m coppers wide and the charged stripes are n coppers wide. In the array calculation, no competing order was introduced on the charged stripes, so the QSE provides the only gap. Figure 5 shows that there is a very good match for both 2 Cu wide and 6 Cu wide stripes, although for the 2 Cu stripe,

the VHS gap is somewhat larger for the single stripe than in the array. From Eq. 10, the 1d bands have dos peaks at band bottom and top; the band bottom corresponds to $k_y = 0$ – i.e., the dispersion from $\Gamma \rightarrow X$ is flat, at the energy corresponding to the lower dos peak. (The intensity along $\Gamma \rightarrow X$ is given by a structure factor, which does not directly come into a single stripe calculation.) Along $X \rightarrow S$ one should see the 1d dispersion extrapolating to the band top at $S = (\pi, \pi)$. Given the good agreement, it should be possible to analyze competing orders on a single stripe, for which the calculations are simpler (no need to self-consistently adjust doping on each row to account for charging effects).

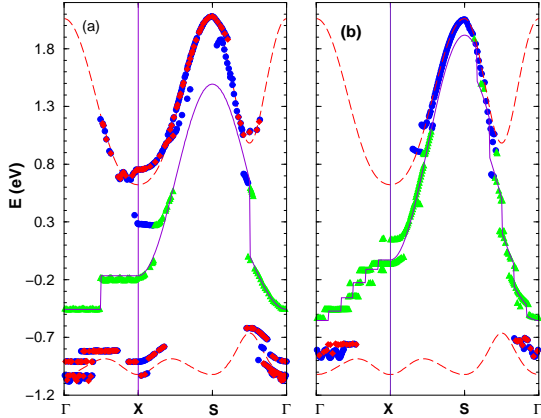


FIG. 5. Dispersion of stripe arrays: (a) (6,2) array with charged stripes 2 Cu wide (AFM stripes 6 Cu wide); (b) (2,6) array with charged stripes 6 Cu wide (AFM stripes 2 Cu wide). Data from Figs. 7a and 7d respectively of Ref. 9; triangles (diamonds) = predominantly from charged (AFM) stripes, while circles = mixed origin; dashed line = Mott bands of AFM stripes; solid line = single (charged) stripe model, with k_x approximated by nearest quantized value.

V. ORDERING ON SINGLE CHARGED STRIPES

A. CDW's and Superconductivity on Paramagnetic Stripes

1. Electron-Phonon Coupling

In this section, we will develop two closely related models of the competition of CDW order and superconductivity *on a single charged stripe*. The first is a Class A paramagnetic stripe, stabilized by electron-phonon coupling^{63,64}, while the second has dominant electron-electron coupling, with (Class B) magnetic charged stripe order.

The earlier calculation⁶³ used a van Hove stabilized CDW model to describe the doping dependence of the pseudogap. Here we reapply the model for a single stripe, by introducing the following modifications. (1) The calculation is carried out on a single, finite width stripe. (2)

Pinning to the VHS arises naturally, since all stripes are at the same doping. (3) For closer approximation to experiment, d-wave superconductivity is assumed. (4) Correlation effects due to Hubbard U are neglected: previous slave boson calculations suggest that the main effect is a bandwidth renormalization of a factor ~ 2 .⁴⁸

We briefly recall the energy dispersion and the gap equations of the model⁶³, generalized to d-wave. In terms of a function

$$\Theta_{\vec{k}} = \begin{cases} 1, & \text{if } |\epsilon_{\vec{k}} - \epsilon_F| < \hbar\omega_{ph}; \\ 0, & \text{otherwise,} \end{cases} \quad (12)$$

the gap functions are $\Delta_{\vec{k}} = \Delta_0 \Theta_{\vec{k}}(c_x - c_y)/2$ for superconductivity, and $G_{\vec{k}} = G_0 + G_1 \Theta_{\vec{k}} \Theta_{\vec{k}+\vec{Q}}$ for the CDW. The energy eigenvalues are $E_{\pm, k}$ and their negatives, with

$$E_{\pm, k}^2 = \frac{1}{2}(E_k^2 + E_{k+Q}^2 + 2G_k^2 \pm \hat{E}_k^2), \quad (13)$$

$E_k^2 = \epsilon_k^2 + \Delta_k^2$, $\hat{E}_k^4 = (E_k^2 - E_{k+Q}^2)^2 + 4G_k^2 \tilde{E}_k^2$, $\tilde{E}_k^2 = \epsilon_{k+}^2 + (\Delta_k - \Delta_{k+Q})^2$, $\epsilon_{k\pm} = \epsilon_k \pm \epsilon_{k+Q}$, and the nesting vector $Q = (\pi, \pi)$. The gap equations are

$$\Delta = \lambda_{\Delta} \Delta \Sigma_{\vec{k}} \frac{\Theta_{\vec{k}}(c_x - c_y)^2/4}{E_{+,k}^2 - E_{-,k}^2} \times \left(\frac{E_{+,k}^2 - \epsilon_{\vec{k}+\vec{Q}}^2 - \Theta_{\vec{k}+\vec{Q}}[\Delta_{\vec{k}}^2 + G_{\vec{k}}^2]}{2E_{+,k}} \tanh \frac{E_{+,k}}{2k_B T} - \frac{E_{-,k}^2 - \epsilon_{\vec{k}+\vec{Q}}^2 - \Theta_{\vec{k}+\vec{Q}}[\Delta_{\vec{k}}^2 + G_{\vec{k}}^2]}{2E_{-,k}} \tanh \frac{E_{-,k}}{2k_B T} \right), \quad (14)$$

$$G_i = \lambda_G \Sigma_{\vec{k}} \frac{\Theta_i G_{\vec{k}}}{E_{+,k}^2 - E_{-,k}^2} \times \left(\frac{E_{+,k}^2 + \epsilon_{\vec{k}} \epsilon_{\vec{k}+\vec{Q}} - \Delta_{\vec{k}}^2 - G_{\vec{k}}^2}{2E_{+,k}} \tanh \frac{E_{+,k}}{2k_B T} - \frac{E_{-,k}^2 + \epsilon_{\vec{k}} \epsilon_{\vec{k}+\vec{Q}} - \Delta_{\vec{k}}^2 - G_{\vec{k}}^2}{2E_{-,k}} \tanh \frac{E_{-,k}}{2k_B T} \right), \quad (15)$$

with interaction energies λ_{Δ} and λ_G , and $\Theta_0 = \Theta_{\vec{k}} \Theta_{\vec{k}+\vec{Q}}$, $\Theta_1 = 1$.

The CDW-superconducting competition was studied in bulk in Ref. 63. The previous results are recovered for a sufficiently wide stripe (~ 100 Cu wide). For narrower stripes, it is found that the quantum confinement gap severely interferes with alternative gap formation. Figure 6 illustrates how the various gaps vary with stripe width, near $x_0 = 0.25$. The data are plotted vs average doping, assuming a regular stripe array with 2-Cu wide AFM stripes (which do not contribute to the gaps) and N-Cu wide charged stripes of doping x_0 , giving an average hole doping $x = Nx_0/(N+2)$.

The CDW gap is most sensitive to stripe width, but in the narrowest stripes superconductivity is also suppressed (the suppression is stronger for a d-wave gap).

Strong instabilities are possible on the stripes, but they are shifted in doping away from $x_0 = 0.25$. Thus, the CDW instability requires both $E_{\vec{k}}$ and $E_{\vec{k}+\vec{Q}}$ to be near the Fermi level; for a two-cell wide stripe, this is only possible near $x = 0$. On the other hand, superconductivity is possible anywhere, if the coupling is strong enough. For a two-cell wide stripe, the optimal superconductivity arises when the Fermi level is at the *one-dimensional VHS* at the edge of one of the stripe subbands. This depends on t' , and for $t' = -0.276t$ falls at $x = 0.582$ (a larger gap is found on the electron-doped side, $x = -0.376$). It should be noted that, even though the superconductivity is assumed to be d-wave, in general a finite minimum gap is found on the stripe, even when the CDW gap is zero. This is because the vanishing d-wave gap can be sampled only when the point $(\pi/2, \pi/2)$ is sufficiently close to the Fermi surface, which in general requires N to be odd (recall that the allowed values of k_x are integer multiples of $\pi/(N+1)$) or very large.

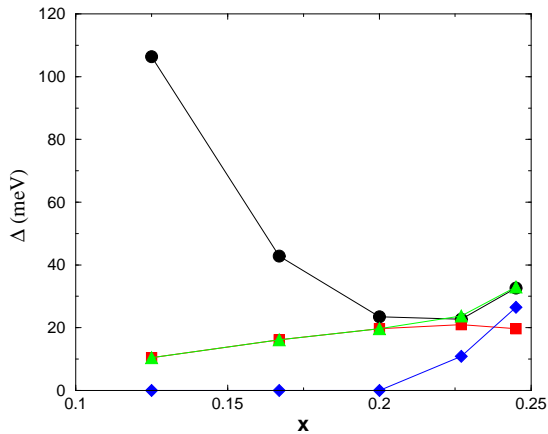


FIG. 6. Gaps on a paramagnetic stripe, as a function of doping (equivalently: stripe width), assuming $x_0 = 0.25$, $\lambda_{CDW} = 0.5eV$, $\lambda_{\Delta} = 0.25eV$. Squares = s-wave superconducting gap; diamonds = CDW gap; triangles = combined gap; circles = total gap at $(\pi, 0)$, including the quantum confinement gap.

2. Electron-Electron Coupling

In the above calculations, the λ 's arose from electron-phonon coupling⁶⁴. Similar contributions follow from electron-electron coupling, in an extended Hubbard model. For instance, the near-neighbor Coulomb repulsion has the following mean-field expansion:

$$V \sum_{\langle i,j \rangle, \sigma, \sigma'} n_{i,\sigma} n_{j,\sigma'} = 4V \sum_{\vec{k}, \sigma} c_{\vec{k}, \sigma}^{\dagger} c_{\vec{k}, \sigma} - 2V \langle O_n \rangle \sum_{\vec{k}, \sigma} (c_x + c_y) c_{\vec{k}, \sigma}^{\dagger} c_{\vec{k}, \sigma}$$

$$\begin{aligned} & -8V \langle T_x \rangle \sum_{\vec{k}, \sigma} c_{\vec{k}+\vec{Q}, \sigma}^{\dagger} c_{\vec{k}, \sigma} \\ & -4V \langle T_y \rangle \sum_{\vec{k}, \sigma} \tilde{\gamma}_k c_{\vec{k}, \sigma}^{\dagger} c_{\vec{k}, \sigma} \\ & +4V \langle T_z \rangle i \sum_{\vec{k}, \sigma} \tilde{\gamma}_k c_{\vec{k}+\vec{Q}, \sigma}^{\dagger} c_{\vec{k}, \sigma} \\ & +4V \sum_{\vec{k}} \tilde{\gamma}_k (\Delta c_{\vec{k}, \uparrow}^{\dagger} c_{-\vec{k}, \downarrow}^{\dagger} + \Delta^* c_{-\vec{k}, \downarrow} c_{\vec{k}, \uparrow}) \\ & +4NV(|\Delta|^2 + \langle O_n \rangle^2 + \langle T_x \rangle^2 + \langle T_y \rangle^2 + \langle T_z \rangle^2), \end{aligned} \quad (16)$$

where $\langle T \rangle^2 = \langle T_x \rangle^2 + \langle T_y \rangle^2 + \langle T_z \rangle^2$ and $\tilde{\gamma}_k = (c_x - c_y)/2$. The first two terms in Eq. 16 renormalize the chemical potential and the hopping t respectively, and can be neglected. The terms in $\langle T_i \rangle$ comprise a pseudospin triplet of CDW-like distortions, with T_x representing a CDW similar to the one discussed above, T_y being related to the low-temperature tetragonal distortion, and T_z an orbital antiferromagnet, closely related to the flux phase. The remaining terms are a d-wave superconductor. The coefficients of the terms must be found self-consistently by solving the gap equations:

$$\sum_{\sigma} \langle c_{i,\sigma}^{\dagger} c_{i,\sigma} \rangle = 1 - x + 2(-1)^{\vec{r}_i} \langle T_x \rangle, \quad (17)$$

$$Im \langle c_{i,\sigma}^{\dagger} c_{i+\hat{x},\sigma} \rangle = -Im \langle c_{i,\sigma}^{\dagger} c_{i+\hat{y},\sigma} \rangle = (-1)^{\vec{r}_i} \langle T_z \rangle, \quad (18)$$

$$\begin{aligned} Re \langle c_{i,\sigma}^{\dagger} c_{i+\hat{x},\sigma} \rangle &= \langle O_n \rangle + \langle T_y \rangle \\ Re \langle c_{i,\sigma}^{\dagger} c_{i+\hat{y},\sigma} \rangle &= \langle O_n \rangle - \langle T_y \rangle, \end{aligned} \quad (19)$$

$$\langle c_{i\uparrow}^{\dagger} c_{i+\hat{x},\downarrow}^{\dagger} \rangle = \Delta. \quad (20)$$

The terms $\langle O_n \rangle$ and $\langle T_y \rangle$ have recently been discussed by Valenzuela and Vozmediano⁶⁵. A detailed discussion of the competition between the three CDW-like modes is given in Ref. 66.

3. d-wave Superconductivity

Retaining only the superconducting term in Eq. 16, the interaction can be derived from a quartic term

$$H' = \sum_{\vec{k}, \vec{l}} V_{\vec{k}, \vec{l}} c_{\vec{k}, \uparrow}^{\dagger} c_{-\vec{k}, \downarrow}^{\dagger} c_{-\vec{l}, \downarrow} c_{\vec{l}, \uparrow}, \quad (21)$$

with $V_{\vec{k}, \vec{l}} = 2V(\cos(k_x - l_x)a + \cos(k_y - l_y)a)$. Assuming $\Delta_{\vec{k}} = \Delta_x \cos k_x a + \Delta_y \cos k_y a$, the gap equations can be written in the form

$$\Delta_i = \sum_{j=x,y} A_{i,j} \Delta_j \quad (22)$$

($i = x, y$), with

$$A_{i,j} = -2V \sum_{\vec{l}} \cos l_i a \cos l_j a \frac{\tanh E_{\vec{l}}/2k_B T}{2E_{\vec{l}}}, \quad (23)$$

and $E_{\vec{l}} = \sqrt{(\epsilon_{\vec{l}} - e_F)^2 + \Delta_{\vec{l}}^2}$.

For the uniform charged state (infinitely wide stripe) $A_{x,x} = A_{y,y}$, and the gap symmetry can be simply analyzed. The symmetry can be either d-wave ($\Delta_y = -\Delta_x$) or extended s-wave ($\Delta_y = +\Delta_x$), with the choice $A_{x,y}\Delta_x\Delta_y > 0$ giving the largest gap. The $A_{x,x}$ term is always BCS-like, having the opposite sign from V , while the $A_{x,y}$ term has the opposite sign from $A_{x,x}$, the integral being dominated by the regions near the VHS's. Hence, there are two possibilities: (i) attractive ($V < 0$) d-wave superconductivity or (ii) repulsive ($V > 0$) extended s-wave. However, the latter would require $|A_{x,y}| > |A_{x,x}|$, which does not arise in the present model, so only case (i) is possible. These considerations readily generalize to a finite-width stripe, for which $A_{x,x} \neq A_{y,y}$.

Agterberg, et al.⁶⁷ recently introduced a model for ‘exotic’ superconductivity in multiband superconductors. If the Fermi surface consists of several inequivalent but degenerate pockets, the order parameter can consist of symmetry allowed superpositions of the order parameters of the individual pockets. Equation 23 can be thought of as a form of exotic superconductivity, with the degenerate VHS's playing the role of hole pockets.

B. Modifications due to Magnetic Order

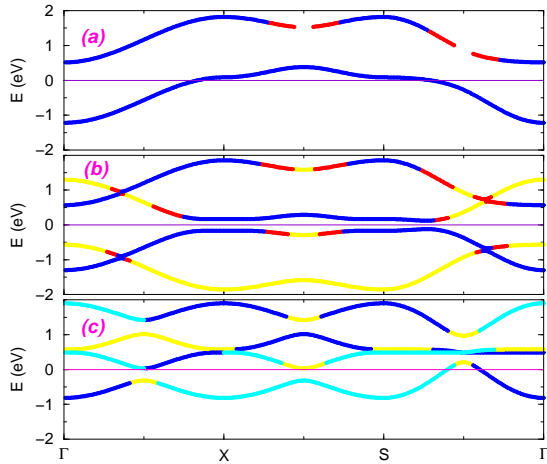


FIG. 7. Dispersion of linear antiferromagnetic (LAF) array along the linear direction (X) (a), along with modifications due to d-wave superconductivity (b) or CDW order (c). $U/t = 6$, $t'/t = 0$, $V/t = 2$ (b), 0.1 (c).

In the above calculations, it was implicitly assumed that the doping is high enough that the only role of the

on-site repulsion U is to renormalize the band parameters. However Baskaran⁶⁸ recently estimated that near optimal doping correlation effects remain stronger than the kinetic energy associated with hopping. Hence, it is important to look for stripe ground states which minimize this on-site repulsion (Class B stripes). The linear antiferromagnet (LAF) stripes discussed in Section III are a good candidate for the cuprate charged stripes: they closely resemble the White-Scalapino stripes¹³, have an appropriate doping, close to $x_0 = 0.25$, include strong correlations, and have the additional advantage that a two-cell wide LAF charge stripe acts as a natural APB for the AF stripes. In this Section, we will explore these stripes, and show that they can be further stabilized by additional interactions.

A special form of strongly correlated CDW is found to exist on a LAF. The charge and spin distribution is shown in the insert to Fig. 8, with the corresponding dispersion in Figure 7c. There is a strong antiferromagnetic ordering on one sublattice, while most of the holes are confined on the other, nonmagnetic sublattice. Whereas in a conventional CDW the charge density is zero on one sublattice and two on the other, in this strong coupling case the hole density varies from 0 to 1, and there is no double occupancy, Fig. 8. Whereas the paramagnetic stripes were extremely sensitive to quantum confinement, these magnetic charged stripes are much less so: this CDW is stable almost independently of the stripe width. From Fig. 7c, it can be seen that the gapped Fermi surface still has hole pockets near $(\pi/2, \pi/2)$, which would lead to conducting stripes, consistent with optical properties⁶⁹. However, it is only found near a hole doping $x = 0.5$, and so does not appear to be relevant for stripe physics in the cuprates.

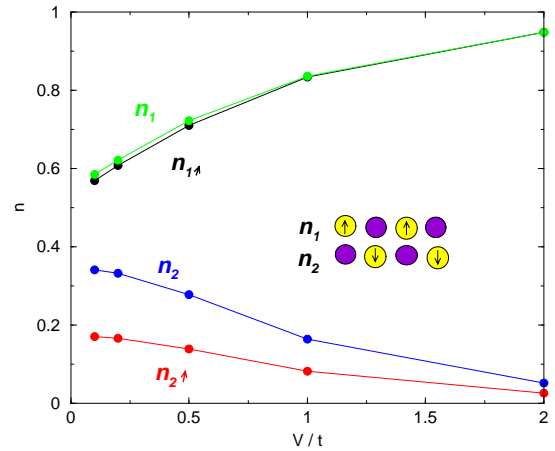


FIG. 8. Linear antiferromagnetic (LAF) array with CDW, showing spin and doping distribution on different sites as a function of interaction strength V , with $U/t = 6$, $t'/t = -0.276$. Inset shows arrangement of atoms.

Away from this doping, CDW instabilities are rela-

tively weak and it is possible to stabilize d-wave superconductivity, Figs. 7b,9. While the overall dispersion varies with stripe width, the superconducting gap is also relatively insensitive to the width, and actually increases for the narrowest stripes, Fig. 10. Note that the order parameter is not a pure d-wave, the gap along the stripe being larger. Such a large anisotropy is not consistent with tunneling measurements of the gap; it is possible that the anisotropy is reduced by strong interstripe coupling. On the other hand, a large gap anisotropy has been found in YBCO⁷⁰, where the stripes are aligned along the chain direction³.

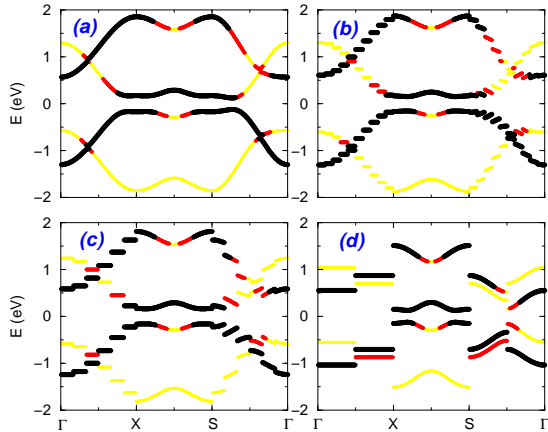


FIG. 9. Dispersion of a LAF with d-wave superconducting order for a uniform system (a) or a single stripe of width $N = 10$ (b), 6 (c), or 2 (d) atoms. Darkness of line reflects relative intensity of dispersion feature.

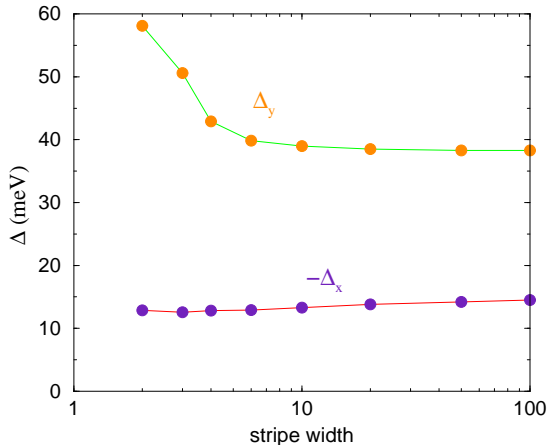


FIG. 10. Linear antiferromagnetic (LAF) array with 'd-wave' superconductivity, showing magnitude of gap along (y) or across (x) the stripes, as a function of stripe width.

Note in Figs. 7b, 9 that the combination of LAF and d-wave order leads to a finite minimum gap over the full Fermi surface. While the pure LAF phase is not stabi-

lized by the VHS, the d-wave superconductivity is optimized when the Fermi level is at the $(\pi, 0)$ VHS – at essentially the *same doping*, $x_0 = 0.245$, as the VHS on a paramagnetic stripe!

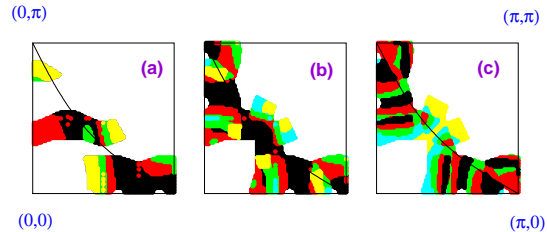


FIG. 11. Constant energy cuts of photoemission dispersion for a (2,2) stripe array, within 200 meV of the Fermi level. Lines = Fermi surface of bulk (or very wide) charged stripes. Relative intensity increases with darker shading. (a) Representative of single domain sample; (b) for multidomain sample (symmetrized about the zone diagonal; (c) with diagonal-suppressing matrix element, $M = |c_x - c_y|$.

VI. EXTENSION TO ARRAYS

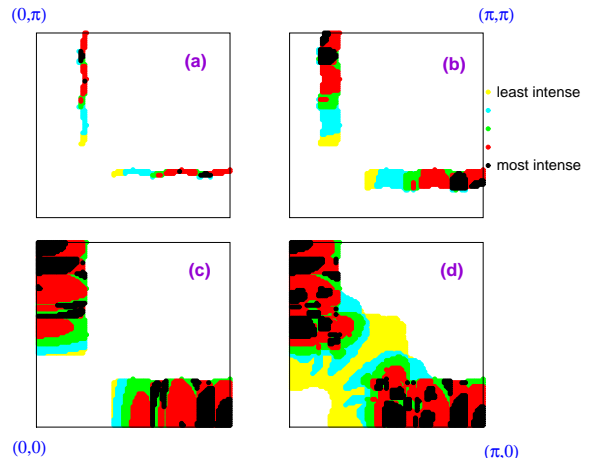


FIG. 12. Constant energy cuts of photoemission dispersion for a (2,2) stripe array, with LAF charged stripes, within (a) 30 (b) 100, (c) 200, or (d) 500 meV of the Fermi level.

In Ref. 9, the Fermi surface was calculated for a series of ordered stripe arrays. These results can now be compared to experimental photoemission data⁷¹. For this purpose we replot the data as integrated spectral weight over a finite energy cut within energy ΔE of the Fermi surface. Figure 11a shows a cut with $\Delta E = 200\text{meV}$, for the model of a 1/8 doped stripe array (i.e., $x = 0.125$)⁹. The pattern is readily understood: the stripe superlattice leads to a number of quasi-one-dimensional bands; however, due to structure factor effects they have significant intensity only near the original Fermi surface, solid line in Fig. 11a. For comparison with experiment, the cal-

culated spectral weight is symmetrized $(0, \pi) \leftrightarrow (\pi, 0)$ in Fig. 11b to represent a sample with regions of stripes running along both X and Y directions. Finally, an empirical matrix element is included, Fig. 11c, which extinguishes spectral weight along the zone diagonal, $(0, 0) \rightarrow (\pi, \pi)$, similar to the matrix element assumed in analyzing Bi2212, Refs. 71,72. The resulting Fermi surface maps for several values of ΔE are illustrated in Ref. 12 for paramagnetic charged stripes, and in Figs. 12 ($x = 1/8$) and 13 ($x = 0.1875$) for LAF stripes.

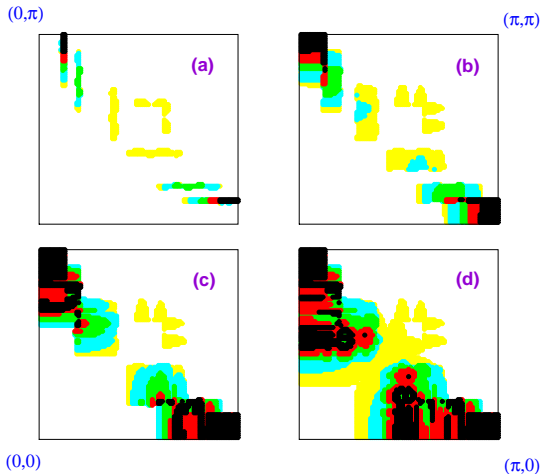


FIG. 13. Constant energy cuts of photoemission dispersion for a (2,6) stripe array, with LAF charged stripes, within (a) 30 (b) 100, (c) 200, or (d) 500 meV of the Fermi level.

For both models, the stripe band nearest $(\pi, 0)$ is in good agreement with experiment: there is little dispersion perpendicular to the stripe, while the intensity falls off toward $(0, 0)$ due to the structure factor effect. In general, the LAF stripes are in better agreement with experiment, since the additional subbands predicted for paramagnetic stripes (moving from $(\pi, 0)$ toward $(0, \pi)$) are not seen in the experiment. While the matrix element improves the agreement, theory suggests that this effect is present only for certain photon polarizations⁷³. One disagreement with experiment for both models is that for shallow energy cuts (30, 100 meV) the experiment still finds a smeared dispersion rather than a sharp Fermi surface. This is presumably an effect of stripe fluctuations.

It should be noted that all the spectral weight in Figs. 11-13 is associated with the charged stripes; the lower Hubbard band of the AFM stripes lies below 0.5eV in LSCO. It is somewhat surprising that the spectral weight nearest the Fermi level is near $(\pi, 0)$, since this is where the pseudogap arises. Nevertheless, our calculation reproduces both the (quantum confinement) pseudogap, Fig. 5, and the spectral weight distribution.

VII. DISCUSSION

A. Additional Evidence for Phase Separation

1. Termination of Stripes

The two most common interpretations for the pseudogap are in terms of either precursor pairing or a competing order parameter, which may be magnetic^{74,75} or charge-density wave (CDW)^{48,76}. We will argue in the next subsection that the latter possibility is more likely. Such competing instabilities arise naturally in a phase separation model (e.g., Refs. 77,9), and we have long argued that the pseudogap is a manifestation of local phase separation⁷⁸. It should be noted that a pseudogap arises in the nickelates⁷⁹ in conjunction with stripe fluctuations, and turns into a true gap at the charge ordering temperature. Therefore, the fact that the pseudogap closes in the overdoped regime in the cuprates strongly suggests that the stripe phase terminates at the same doping. Direct evidence for this has recently appeared^{19,6,80,3}. Figure 14a compares the intensity I of the inelastic neutron peaks near (π, π) as a function of doping in YBCO⁸¹ and LSCO^{2,1}. In a stripe picture, I should be a measure of the fraction of material in AFM stripes. Remarkably, the intensity extrapolates to zero at nearly the same doping in both materials, even though $T_c(x)$ peaks at substantially different dopings. For both materials, this is the doping at which the pseudogap closes. While in YBCO, these peaks have been interpreted as a Fermi surface nesting effect^{82,83}, this cannot explain the charge order fluctuations, and in LSCO the Tranquada data² is associated with *elastic* magnetic peaks. Furthermore, a study of the neutron diffraction pair distribution function⁸⁴ for LSCO finds evidence for charge fluctuations, presumably associated with stripes. The excess fluctuations are maximal near $x = 0.15$, and terminate near $x = 0.25$. Strong reductions of thermal conductivity associated with stripe scattering also terminate at a comparable doping⁸⁵, while a recent optical study⁸⁶ finds evidence for a quantum critical point at a similar doping, $x \sim 0.22$. Moreover, in Bi2212, Tokunaga, et al.⁸⁷ have introduced a new crossover temperature T_{mK} based on Cu NMR, below which AFM correlations develop; they find $T_{mK} \rightarrow 0$ near $x = 0.26$.

A recent NQR study of the slowing of spin fluctuations in RE substituted LSCO⁸⁸ finds that the effective spin stiffness ρ_s^{eff} (or equivalently the effective exchange constant) scales to zero at a comparable doping; the inverted triangles in Fig. 14 show $2\pi\rho_s^{eff}/460K$. As might have been anticipated from Sections II,IV, the doping dependence of ρ_s^{eff} changes radically below $x = 0.12$. Note that while the integrated neutron intensity scales approximately with the area fraction of charged stripes, $2\pi\rho_s^{eff}$ scales to $\sim 460K$ as $x \rightarrow 0$. This is only 1/4 of the actual spin stiffness, $2\pi\rho_s = 1.13J = 1730K$ in the undoped AFM. The change by nearly a factor of four is suggestive of a dimensional reduction (lower coordination), but for an isolated straight spin ladder, a factor of two might

have been expected.

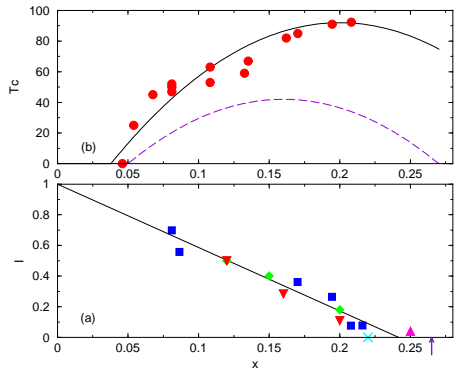


FIG. 14. (a) Magnetic inelastic scattering intensity vs x in YBCO (squares⁸¹) and LSCO (diamonds² and triangle¹). Inverted triangles = (scaled) effective exchange constant in RE substituted LSCO, estimated from slowing of spin fluctuations⁸⁸. (b) Corresponding $T_c(x)$: solid line = YBCO (circles⁸¹); dashed line = LSCO.

It is important to note the proximity of this termination of the phase separation regime to the VHS: the arrow in Fig. 14a shows the doping at which the pseudogap in the heat capacity⁸⁹ closes, leaving an approximately logarithmic peak⁵², while the \times indicates the point at which photoemission finds the VHS crossing the Fermi level⁹⁰. Termination of the stripe phase close to a VHS is an important prediction of our EPS model of stripes.

Figure 14 has a bearing on the discussion given earlier of optimal doping in YBCO, or equivalently of the doping x at which the stripe phase terminates. Setting optimal doping at $x = 0.16$ for all cuprates puts the termination at doping $x_0 = 0.19$. However, this value is clearly too low for LSCO: when the stripes are gone, magnetic correlations should be weak, but there is evidence for long range magnetic order at $x = 0.2^2$ and 0.21 , the latter coupled with a suppression of T_c ⁹¹. On the other hand, both facts are compatible with $x_0 \sim 0.25$, Fig. 14.

The termination of the pseudogap has also been interpreted in terms of a quantum critical point (QCP)^{92,8}. At first glance, it looks straightforward to distinguish a model of EPS, which is by nature first order, from a QCP, which is typically second order. However, the phases are actually quite similar. Due to strong coulomb effects, the EPS is restricted to nanoscopic scale, so that, e.g., the superconducting critical temperature T_c changes smoothly with doping. On the other hand, near a QCP with quenched disorder, long-time correlations can lead to effective spatial inhomogeneity⁹³.

2. Doping Dependence of Charged Stripes and Superconductivity

We suggested earlier⁹ that the peak and hump features seen in photoemission from Bi2212 were associated with the charged and the AFM stripes respectively. As such, the intensity of the peak should have the doping dependence predicted for charged stripes, with the intensity increasing from zero at half filling, approximately linearly with doping x . This has now been verified experimentally^{90,94}. Moreover, the maximum intensity of the spectral weight occurs at the same doping⁹⁰ x_0 discussed above, where the stripe phase terminates. Remarkably, the peak spectral weight closely tracks T_c , suggesting that *the superconducting pairs live on the charged stripes*, as predicted by several models^{52,95}. Consistent with this, a number of measures of the strength of superconductivity (condensation energy, critical current) are optimized at this same point^{90,6,96} where the charge stripe intensity is maximum and AFM stripes vanish. The fact that T_c itself is actually optimized at a slightly lower doping may be a hint that stripes can enhance the superconducting gap, as found above, Fig. 10.

The sharp falloff of spectral weight at higher doping may be an indication for a *second regime of phase separation* in overdoped samples, where the new phase is not intrinsically superconducting. Some additional evidence for such a phase separation is discussed below.

3. Second Regime of Phase Separation

It is important to note that as soon as the pseudogap closes, experiments find a peak in the density of states consistent with that expected for a VHS. This is discussed in Ref. 52 on p. 1203 (Fig. 21); more recent evidence is in Ref. 97. For even higher dopings there are hints of a new regime of phase separation. This is an important prediction of the model: if stripes are stabilized by lowering the electronic energy at a VHS, then there could be a *second range of phase separation* in the overdoped regime, with the non-superconducting phase totally unrelated to the AFM state at half filling.

Earlier experimental evidence for this second regime of phase separation in the cuprates has been presented in References 52 (Section 11.6) and 98 (see also Wen, et al⁹⁹). Recently, Loram⁸⁹ has presented a detailed analysis of the heat capacity of $\text{La}_{2-x}\text{Sr}_x\text{CuO}_4$ over an extended doping range. In the range $0.26 < x < 0.3$, the temperature dependence of the Sommerfeld constant γ is consistent with that expected for a uniform phase close to a VHS (Ref. 52, Fig. 21). For lower doping, γ falls off too rapidly to be associated with rigid-band filling away from a VHS, but can be easily explained in terms of the opening of a pseudogap. For higher hole doping, γ again falls off¹⁰⁰ too rapidly to be due to rigid band filling, although without an obvious pseudogap form-

ing. The near symmetry of γ between the overdoped and underdoped sides is suggestive of two regimes of phase separation. Further possible evidence for this second regime comes from tunneling studies¹⁰¹ which find a subdominant order parameter in optimally and overdoped YBCO (i.e., in the same doping range where a split superconducting transition is found¹⁰²). This could arise from an Allender-Bray-Bardeen mechanism¹⁰³, with the d-wave superconducting stripes inducing s-wave (or d_{xy}) superconductivity on adjacent normal-Fermi-metal stripes. Also, microwave measurements⁵ find a crossover near optimal doping from superconductor-insulator to superconductor-metal domains.

Uemura¹⁰⁴ has also recently proposed phase separation in the overdoped cuprates. In extending the Uemura plot to the overdoped regime, a ‘boomerang’ effect is found: both T_c and n_s/m decrease in parallel¹⁰⁵. Here n_s is the superfluid density and m is the effective mass, and their ratio is extracted from μ SR measurements of the penetration depth. Uemura¹⁰⁴ suggests that this proportionality between T_c and n_s/m can most easily be accounted for in terms of (nanoscale) phase separation between the superconductor and a non-superconducting phase. Thus for both overdoped and underdoped cuprates¹⁰⁶, the scaling between T_c and n_s can be understood in terms of phase separation. This has important implications for superconductivity: *superconductivity arises only at a unique composition near optimal doping*. The present results suggest that even at this doping, the superconductivity must compete with a second order parameter.

B. Superconducting Fluctuations

Above, we have presented evidence that the optimum T_c occurs at a different doping in LSCO than for the other cuprates, while the stripes terminate at approximately the same doping for all cuprates. Further evidence for this can be found by comparing the superconducting fluctuations^{107–110,87}, Fig. 15. In all three materials, LSCO, YBCO, and Bi2212, some superconducting fluctuations appear to persist in the low doping regime, to temperatures in excess of optimal T_c (although considerably less than the pseudogap temperature). The fluctuating superconductivity in LSCO is very similar to that found in the other cuprates. On the other hand, if one assumed a universal curve of superconductivity, with $T_c/T_{c,max}$ vs x the same for all cuprates, then the scaled superconducting fluctuations in LSCO would be at anomalously high temperatures. It seems simpler to assume that in LSCO long range superconducting order is anomalously suppressed (as also suggested by Baskaran¹¹¹), in which case there is no reason for optimal T_c to fall at the same doping.

In Bi2212 and YBCO, the onset of superconducting fluctuations falls close to the ‘strong pseudogap’ regime^{112,113}, and hence at temperatures substantially

below the weak pseudogap temperature^{114,115}, making it unlikely that the weak pseudogap is associated with preformed pairs. In LSCO, there is some confusion, since the pseudogap temperatures reported by Batlogg, et al.¹¹⁴ are considerably higher than those found by Ido, et al.¹¹⁵. The Ido T^* ’s fall close to the fluctuation onset temperatures in Fig. 15.

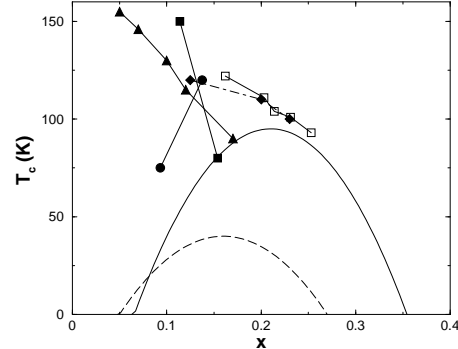


FIG. 15. Doping dependence of T_c (solid line for YBCO, Bi2212, dashed line for LSCO) and superconducting fluctuations in Bi2212 (circles) [107] and (diamonds) [87], LSCO (triangles) [108], and YBCO (closed squares) [109] and (open squares) [110].

The fluctuations observed in Fig. 15 are very suggestive of the theoretical results of Fig. 10: thus, quantum size effects enhance the average gap on a narrow stripe, which will lead to an enhanced mean field transition temperature in the underdoped regime. However, the coupling between stripes also weakens, leading to a loss of interstripe coherence, so the pairing is only evident as enhanced fluctuations.¹¹⁶

VIII. CONCLUSIONS

Recent experiments have provided considerable evidence for the presence of stripes and EPS in the cuprates, but there remain many questions of how universal these are, how they arise and vary with doping, and how they interact with superconductivity. We have here elaborated our earlier⁹ model of stripes driven by frustrated phase separation, in particular adducing evidence that the doping on the charged stripes is close to $x = x_0 = 0.25$, and that when the average doping approaches this value EPS terminates. Moreover, near $x_{cr} = x_0/2$ there is a crossover in stripe properties: for $x < x_{cr}$ the charged stripes are quantum confined, for $x > x_{cr}$ the AFM stripes are so confined. This model can explain the 1/8 anomaly ($x = x_{cr}$), the anomalous Hall effect ($R_H \rightarrow 0$)²⁴ for $x < 1/8$ (charged stripes confined, hence one-dimensional), and the growing spin gap in YBCO for $x > 1/8$ ⁹.

On the important issue of the *structure* of a charged stripe, we have explored a number of possibilities without

coming to any final conclusions. While there is evidence that superconductivity lives on the charged stripes, there also appears to be a second instability on these stripes, which stabilizes the stripe phase while competing with superconductivity. We have shown that a semiquantitative understanding can be achieved by looking at the properties of a single doped ladder, and we have discussed how a number of instabilities (both CDW and superconducting) vary with ladder width. We showed that strong correlation effects could lead to charged stripes with a residual magnetic order, introduced a simple model for White-Scalapino-like stripes, and found novel superconducting and CDW instabilities associated with such stripes. We illustrated how stripe order would affect ARPES spectra, both dispersions and Fermi surface maps. Future studies will apply the model to describing other properties of the cuprates.

Certain anomalous features of strong-correlation calculations may find an explanation in underlying phase separation. Thus, the vanishing of the renormalized hopping parameter t near half filling in slave boson calculations may reflect the vanishing of the charged stripes at half filling⁹, while the frequently-observed pinning of the VHS near the Fermi level^{52,117} is consistent with VHS-stabilized charged stripes.

Finally, the idea of a commensurability effect near $1/8$ doping, leading to a coexistence of *domains* for $x > 1/8$, provides a simple explanation for a large variety of experimental findings, including the saturation of the Yamada plot, the direct observation of domains in STM studies, and a variety of microwave anomalies. This may also lead to a resolution of the combined puzzle of magnetic neutron scattering incommensurability and the neutron resonance peak. A stripe model provides a natural explanation of the incommensurability for $x \leq 1/8$, including a stripe reorientation transition at the metal-superconductor transition near $x \sim 0.053$. However, a band picture⁸³ (with E_F close to a VHS) provides a superior model for the combined, frequency-dependent incommensurability *cum* resonance peak found near optimal doping in YBCO and Bi2212. An EPS crossover from stripes to domains near $x \sim 1/8$ would provide a natural explanation of these phenomena. Interestingly, the only calculation⁸² to approximately describe the doping dependence is based on a slave boson model, which as noted above tends to mimic EPS behavior as $x \rightarrow 0$.

Acknowledgment: These computations were carried out using the facilities of the Advanced Scientific Computation Center at Northestern University (NU-ASCC). Their support is gratefully acknowledged. We had stimulating conversations with S. Pan and J.C. Davis. CK's research was supported in part by NSF Grant NSF-9711910. Publication 776 of the Barnett Institute.

- ¹ K. Yamada, C.H. Lee, K. Kurahashi, J. Wada, S. Wakimoto, S. Ueki, H. Kimura, Y. Endoh, S. Hosoya, G. Shirane, R.J. Birgeneau, M. Greven, M.A. Kastner, and Y.J. Kim, Phys. Rev. B **57**, 6165 (1998).
- ² J.M. Tranquada, B.J. Sternlieb, J.D. Axe, Y. Nakamura, and S. Uchida, Nature **375**, 561 (1995); J.M. Tranquada, J.D. Axe, N. Ichikawa, A.R. Moodenbaugh, Y. Nakamura, and S. Uchida, Phys. Rev. Lett **78**, 338 (1997).
- ³ H.A. Mook, presented at the Sixth International Conference on the Materials and Mechanisms of Superconductivity – High-Temperature Superconductivity (M²S-HTSC-VI), Houston, TX, Feb. 20-25, 2000; H.A. Mook and F. Doğan, Nature **401**, 145 (1999), and cond-mat/0103037.
- ⁴ T. Cren, D. Roditchev, W. Sacks, J. Klein, J.-B. Moussy, C. Deville-Cavellin, and M. Laguès, Phys. Rev. Lett. **84**, 147 (2000); C. Howald, P. Fournier, A. Kapitulnik, cond-mat/0101251; S.H. Pan, J.P. O'Neal, R.L. Badzey, C. Chamon, H. Ding, J.R. Engelbrecht, Z. Wang, H. Eisaki, S. Uchida, A.K. Gupta, K.-W. Ng, E.W. Hudson, K.M. Lang, and J.C. Davis, unpublished; and J.C. Davis, presented at the Sixth Internat. Conf. on Spectroscopies of Novel Superconductors (SNS01), Chicago, May 13-17 (2001), unpublished.
- ⁵ J. Orenstein, presented at SNS01, unpublished.
- ⁶ J.L. Tallon, cond-mat/9911422, J.L. Tallon, J.W. Loram, and G.V.M. Williams, cond-mat/9911423, J.L. Tallon, J.W. Loram, G.V.M. Williams, J.R. Cooper, I.R. Fisher, J.D. Johnson, M.P. Staines, and C. Bernhard, Phys. Stat. Sol. **b215**, 531 (1999).
- ⁷ M.I. Salkola, V.J. Emery, and S.A. Kivelson, Phys. Rev. Lett. **77**, 155 (1996).
- ⁸ S. Caprara, C. Di Castro, M. Grilli, A. Perali, and M. Sulpizi, Physica **C317-8**, 230 (1999); G. Seibold, F. Becca, F. Bucci, C. Castellani, C. di Castro, and M. Grilli, cond-mat/9906108.
- ⁹ R.S. Markiewicz, Phys. Rev. B **62**, 1252 (2000).
- ¹⁰ M.G. Zacher, R. Eder, E. Arrighi, and W. Hanke, Phys. Rev. Lett. **85**, 2585 (2000).
- ¹¹ J. Eroles, G. Ortiz, A.V. Balatsky, and A.R. Bishop, cond-mat/0008341.
- ¹² R.S. Markiewicz and C. Kusko, Int. J. Mod. Phys. **B14**, 3561 (2000).
- ¹³ S.R. White and D.J. Scalapino, Phys. Rev. Lett. **80**, 1272 (1998), *ibid.* **81**, 3227 (1998).
- ¹⁴ M.V. Zimmermann, A. Vigliante, T. Niemöller, N. Ichikawa, T. Frello, J. Madsen, P. Wochner, S. Uchida, N.H. Andersen, J.M. Tranquada, D. Gibbs, and J.R. Schneider, Europhys. Lett. **41**, 629 (1998); T. Niemoeller, N. Ichikawa, T. Frello, H. Huennefeld, N.H. Andersen, S. Uchida, J.R. Schneider, and J.M. Tranquada, cond-mat/9904383; T. Niemöller, H. Hünnefeld, T. Frello, N.H. Andersen, N. Ichikawa, S. Uchida, and J.R. Schneider, J. Low-T. Phys. **117**, 455 (1999).
- ¹⁵ K.M. Kojima, H. Eisaki, S. Uchida, Y. Fudamoto, I.M. Gat, A. Kinkhabwala, M.I. Larkin, G.M. Luke, and Y.J. Uemura, Physica **B289-90**, 343 (2000).
- ¹⁶ G.B. Teitelbaum, B. Büchner, and H. de Gronkel, Phys. Rev. Lett. **84**, 2949 (2000).
- ¹⁷ J. Tworzydło, C.N.A. van Duin, and J. Zaanen, Proc. of 2nd Intern. Conf. on Stripes and High Tc Superconductivity

- tivity, Rome '98, to be published, J. Supercond. (cond-mat/9808034).
- ¹⁸ J.L. Tallon, Physica C **168**, 85 (1990).
- ¹⁹ Y.J. Uemura, G.M. Luke, B.J. Sternlieb, J.H. Brewer, J.F. Carolan, W.N. Hardy, R. Kadano, J.R. Kempton, R.F. Kiefl, S.R. Kreitzman, P. Mulhern, T.M. Riseman, D.Ll. Williams, B.X. Yang, S. Uchida, H. Takagi, J. Gopalakrishnan, A.W. Sleight, M.A. Subramanian, C.L. Chien, M.Z. Cieplak, G. Xiao, V.Y. Lee, B.W. Statt, C.E. Stronach, W.J. Kossler, and X.H. Yu, Phys. Rev. Lett. **62**, 2317 (1989).
- ²⁰ Optical evidence that x and the superelectron density n_s both scale with T_c is found in H.L. Liu, M.A. Quijada, A. Zibold, Y.-D. Yoon, D.B. Tanner, G. Cao, J.E. Crow, H. Berger, G. Margaritondo, L. Forró, Beom-Hoan O, J.T. Markert, R.J. Kelly, and M. Onellion, J. Phys. Cond. Matt. **11**, 239 (1999).
- ²¹ Consistent with $x_{opt} = 0.21$ [Y. Tokura, J.B. Torrance, T.C. Huang, and A.I. Nazzal, Phys. Rev. **B38**, 7156 (1988)], 0.24 [U. Tutsch, P. Schweiss, R. Hauff, B. Obst, Th. Wolf, and H. Wühl, J. Low-T. Phys. **117**, 951 (1999)], 0.2 [M. Merz, N. Nücker, P. Schweiss, S. Schuppler, C.T. Chen, V. Chakarian, J. Freeland, Y.U. Idzerta, M. Kläser, G. Müller-Vogt, and Th. Wolf, Phys. Rev. Lett. **80**, 5192 (1998)], 0.21 [S.L. Drechsler, J. Malek, and H. Eschrig, Phys. Rev. **B55**, 606 (1997)]. A recent critique of Tallon's bond valence sum calculation¹⁸ also finds evidence for a larger x_{opt} , but concludes that the technique cannot accurately determine the mobile hole fraction on the CuO₂ planes [O. Chmaissem, Y. Eckstein, and C.G. Kuper, Phys. Rev. **B63**, 174510 (2001).]
- ²² J.L. Tallon, J.R. Cooper, P.S.I.P.N. de Silva, G.V.M. Williams, and J.W. Loram, Phys. Rev. Lett. **75**, 4114 (1995).
- ²³ E.C. Jones, D.C. Christen, J.R. Thompson, R. Feenstra, S. Zhu, D.H. Lowndes, J.M. Phillips, M.P. Siegal, and J.D. Budai, Phys. Rev. **B47**, 8986 (1993).
- ²⁴ T. Noda, H. Eisaki, and S. Uchida, Science **286**, 265 (1999).
- ²⁵ V. Kataev, B. Rameev, A. Validov, B. Büchner, M. Hücker, and R. Borowski, Phys. Rev. **B58**, 11876 (1998).
- ²⁶ S. Sugai and N. Hayamizu, J. Phys. Chem. Solids **62**, 177 (2001).
- ²⁷ G. Blumberg, M.V. Klein, and S.-W. Cheong, Phys. Rev. Lett. **80**, 564 (1998); K. Yamamoto, T. Katsufuji, T. Tanabe, and Y. Tokura, Phys. Rev. Lett. **80**, 1493 (1998); and S. Sugai, N. Kitamori, S. Hosoya, and K. Yamada, J. Phys. Soc. Jpn. **67**, 2992 (1998).
- ²⁸ M. Fujita, K. Yamada, H. Hiraka, P.M. Gehring, S.H. Lee, S. Wakimoto, and G. Shirane, cond-mat/0101320.
- ²⁹ M. Arai, T. Nishijima, Y. Endoh, A.W. Garrett, S. Tajima, K. Tomimoto, Y. Shiohara, C.D. Frost, and S.M. Bennington, cond-mat/9912233; M. Arai, Y. Endoh, S. Tajima, and S.M. Bennington, Int. J. Mod. Phys. **B14**, 3312 (2000).
- ³⁰ P. Dai, H.A. Mook, R.D. Hunt, and F. Dogan, Phys. Rev. **B63**, 54525 (2001).
- ³¹ A. Ino, T. Mizokawa, A. Fujimori, K. Tamasaku, H. Eisaki, S. Uchida, T. Kimura, T. Sasagawa, and K. Kishio, Phys. Rev. Lett. **79**, 2101 (1997).
- ³² M. Satake, K. Kobayashi, T. Mizokawa, A. Fujimori, T. Tanabe, T. Katsufuji, and Y. Tokura, Phys. Rev. **B61**, 15515 (2000).
- ³³ A.V. Balatsky, presented at SNS01, unpublished.
- ³⁴ A. Erb, A.A. Manuel, M. Dhalle, F. Marti, J.-Y. Genoud, B. Revaz, A. Junod, D. Vasumathi, S. Ishibashi, A. Shukla, E. Walker, O. Fischer, R. Fluekiger, R. Pozzi, M. Mali, and D. Brinkmann, Sol. St. Commun. **112**, 245 (1999).
- ³⁵ O. Fischer, presented at SNS01, unpublished.
- ³⁶ P.C. Hammel, A.P. Reyes, S.-W. Cheong, Z. Fisk, and J.E. Schirber, Phys. Rev. Lett. **71**, 440 (1993).
- ³⁷ C. Kusko, Z. Zhai, N. Hakim, R.S. Markiewicz, S. Sridhar, D. Colson, Viallet-Guillet, A. Forget, Yu.A. Nefyodov, M.R. Trunin, N.N. Kolesnikov, A. Maignan, A. Daignere, and A. Erb, unpublished; R.S. Markiewicz, unpublished.
- ³⁸ X.J. Zhou, T. Yoshida, S.A. Kellar, P.V. Bogdanov, E.D. Lu, A. Lanzara, M. Nakamura, T. Noda, T. Takeshita, H. Eisaki, S. Uchida, A. Fujimori, Z. Hussain, and Z.-X. Shen, Phys. Rev. Lett. **86**, 5578 (2001).
- ³⁹ J. Zaanen and A.M. Oles, Ann. Physik **5**, 224 (1996); C. Nayak and F. Wilczek, Phys. Rev. Lett. **78**, 2465 (1997); V.J. Emery, S.A. Kivelson, and O. Zachar, Phys. Rev. **B56**, 6120 (1997); S.A. Kivelson, E. Fradkin, and V.J. Emery, Nature **393**, 550 (1998).
- ⁴⁰ M. Ichioka and K. Machida, J. Phys. Soc. Jpn. **68**, 4020 (1999).
- ⁴¹ B. Valenzuela, M. Vozmediano, and F. Guinea, Phys. Rev. **B62**, 11312 (2000), and M. Vozmediano, personal communication.
- ⁴² S. Chakravarty, R.B. Laughlin, D.K. Morr, and C. Nayak, Phys. Rev. **B63**, 94503 (2001); J. Zaanen, cond-mat/0103255.
- ⁴³ M.D. Kaplan and B.G. Vekhter, "Cooperative Phenomena in Jahn-Teller Crystals" (Plenum, N.Y., 1995), p. 216.
- ⁴⁴ J. Hafner, "From Hamiltonians to Phase Diagrams" (Springer, Berlin, 1987).
- ⁴⁵ P.W. Anderson, "Van Hove singularities as a source of anomalies in the cuprates", PUP preprint 414 (1994), and "The Theory of High-T_c Superconductivity", (Princeton, University Press, 1997).
- ⁴⁶ Y.-S. Yi, Z.-G. Yu, A.R. Bishop, and J.T. Gammel, Phys. Rev. **B58**, 503 (1998).
- ⁴⁷ T. Tohyama, S. Nagai, Y. Shibata, and S. Maekawa, Phys. Rev. Lett. **82**, 4910 (1999).
- ⁴⁸ R.S. Markiewicz, Phys. Rev. **B56**, 9091 (1997).
- ⁴⁹ P. Fazekas, Foundations of Physics **30**, 1999 (2000).
- ⁵⁰ C. Kusko and R.S. Markiewicz, unpublished, cond-mat/0102440.
- ⁵¹ R. Hlubina, S. Sorella, and F. Guinea, Phys. Rev. Lett. **78**, 1343 (1997); R. Hlubina, Phys. Rev. **B59**, 9600 (1999). See also D. Vollhardt, N. Blümer, K. Held, M. Kollar, J. Schlipf, and M. Ulmke, Z. Phys. **B103**, 283 (1997).
- ⁵² R.S. Markiewicz, J. Phys. Chem. Sol. **58**, 1179 (1997).
- ⁵³ J. Fritzenkötter and K. Dichtel, in "Stripes and Related Phenomena", ed. by A. Bianconi and N. Saini, (Kluwer Academic/Plenum, N.Y., 2000), p. 369.
- ⁵⁴ P.B. Visscher, Phys. Rev. **B10**, 943 (1974); E.L. Nagaev, "Physics of Magnetic Semiconductors" (Moscow, Mir, 1983).

- ⁵⁵ G. Su, Phys. Rev. B **54**, 8281 (1996); A.C. Cosentini, M. Capone, L. Guidoni, and G.B. Bachelet, Phys. Rev. B **58**, 14685 (1998).
- ⁵⁶ W.O. Putikka, R.L. Glenister, and R.R.P. Singh, Phys. Rev. Lett. **73**, 170 (1994); C.T. Shih, Y.C. Chen, and T.K. Lee, Phys. Rev. B **57**, 627 (1998); and M. Calandra, F. Becca, and S. Sorella, Phys. Rev. Lett. **81**, 5185 (1998).
- ⁵⁷ C.S. Hellberg and E. Manousakis, (a) Phys. Rev. Lett. **78**, 4609 (1997), (b) Phys. Rev. B **61**, 11787 (2000).
- ⁵⁸ L. P. Pryadko, S. Kivelson and D. W. Hone, Phys. Rev. Lett. **80**, 5651 (1998).
- ⁵⁹ H. Schulz, J. Phys. (Paris) **50**, 2833 (1989); D. Poilblanc and T.M. Rice, Phys. Rev. B **39**, 9749 (1989); J. Zaanen and O. Gunnarsson, *ibid.* B **40**, 7391 (1989); M. Inui and P.B. Littlewood, *ibid.* B **44**, 4415 (1991); A. Singh and Z. Tešanović, *ibid.* B **41**, 614 (1990); K. Yonemitsu, A.R. Bishop, and J. Lorenzana, Phys. Rev. B **47**, 8065, 12059 (1993); and D. Góra, K. Rościszewski, and A.M. Oleś, Phys. Rev. B **60**, 7429 (1999).
- ⁶⁰ J.A. Vergés, E. Louis, M.P. López-Sancho, F. Guinea, and A.R. Bishop, Phys. Rev. B **43**, 6099 (1991).
- ⁶¹ M. Kato, K. Machida, H. Nakanishi, and M. Fujita, J. Phys. Soc. Jpn. **59**, 1047 (1990).
- ⁶² R.B. Laughlin, cond-mat/9709195; J. Zaanen, J. Phys. Chem. Solids **59**, 1769 (1998).
- ⁶³ R.S. Markiewicz, C. Kusko and V. Kidambi, Phys. Rev. B **60**, 627 (1999).
- ⁶⁴ C. Balseiro and L. Falicov, Phys. Rev. B **20**, 4457 (1979).
- ⁶⁵ B. Valenzuela and M.A.H. Vozmediano, Phys. Rev. B **63**, 153103 (2000).
- ⁶⁶ R.S. Markiewicz and C. Kusko, unpublished, cond-mat/0102452.
- ⁶⁷ D.F. Agterberg, V. Barzykin, and L.P. Gor'kov, Europhys. Lett. **48**, 449 (1999) and Phys. Rev. B **60**, 14868 (2000).
- ⁶⁸ G. Baskaran, cond-mat/0007137.
- ⁶⁹ R.S. Markiewicz, unpublished.
- ⁷⁰ D.H. Lu, D.L. Feng, N.P. Armitage, K.M. Shen, A. Damascelli, C. Kim, F. Ronning, Z.-X. Shen, D.A. Bonn, R. Liang, W.N. Hardy, A.I. Rykov, and S. Tajima, Phys. Rev. Lett. **86**, 4370 (2001).
- ⁷¹ X.J. Zhou, P. Bogdanov, S.A. Kellar, T. Noda, H. Eisaki, S. Uchida, Z. Hussain, and Z.-X. Shen, Science **286**, 268 (1999).
- ⁷² D. Orgad, S.A. Kivelson, E.W. Carlson, V.J. Emery, X.J. Zhou, and Z.-X. Shen, Phys. Rev. Lett. **86**, 4362 (2001).
- ⁷³ M. Lindroos and A. Bansil, personal communication.
- ⁷⁴ A. Kampf and J. Schrieffer, Phys. Rev. B **41**, 6399 (1990).
- ⁷⁵ S.-C. Zhang, Science **275**, 1089 (1997).
- ⁷⁶ R.A. Klemm, unpublished, and Physica C **341-8**, 839 (2000).
- ⁷⁷ C. Castellani, C. Di Castro, and M. Grilli, Phys. Rev. Lett. **75**, 4650 (1995).
- ⁷⁸ R.S. Markiewicz, Physica C **169**, 63 (1990).
- ⁷⁹ T. Katsufuji, T. Tanabe, T. Ishikawa, Y. Fukuda, T. Arima, and Y. Tokura, Phys. Rev. B **54**, 14230 (1996).
- ⁸⁰ P. Bourges, cond-mat/0009373.
- ⁸¹ P. Bourges, L.P. Regnault, J.Y. Henry, C. Vettier, Y. Sidis, and P. Burlet, Physica B **215**, 30 (1995).
- ⁸² J. Brinckmann and P.A. Lee, Phys. Rev. Lett. **82**, 2915 (1999).
- ⁸³ M.R. Norman, cond-mat/9912203; Y.-J. Kao, Q. Si, and K. Levin, Phys. Rev. B **61**, 11898 (2000).
- ⁸⁴ E.S. Božin, G.H. Kwei, H. Takagi, and S.J.L. Billinge, Phys. Rev. Lett. **84**, 5856 (2000).
- ⁸⁵ O. Baberski, A. Lang, O. Maldonado, M. Hücker, B. Büchner, and A. Freimuth, Europhys. Lett. **44**, 335 (1998).
- ⁸⁶ T. Timusk, A.V. Puchkov, S. Doyle, A.M. Hermann, and N.N. Kolesnikov, unpublished.
- ⁸⁷ Y. Tokunaga, K. Ishida, K. Yoshida, T. Mito, Y. Kitaoka, Y. Nakayama, J. Shimoyama, K. Kishio, O. Narikiyo, and K. Miyake, Physica B **284-88**, 663 (2000).
- ⁸⁸ A.W. Hunt, P.M. Singer, A.F. Cederström, and T. Imai, cond-mat/0011380.
- ⁸⁹ J.W. Loram, J.L. Luo, J.R. Cooper, W.Y. Liang, and J.L. Tallon, Physica C **341-8**, 831 (2000).
- ⁹⁰ Z.X. Shen, presented at M²S-HTSC-VI, Houston, TX, Feb. 20-25, 2000; D.L. Feng, D.H. Lu, K.M. Shen, C. Kim, H. Eisaki, A. Damascelli, R. Yoshizaki, J.-i. Shimoyama, K. Kishio, G. Gu, S. Oh, A. Andrus, J. O'Donnell, J.N. Eckstein, and Z.-X. Shen, Science **280**, 277 (2000).
- ⁹¹ Y. Koike, M. Akoshima, M. Aoyama, K. Nishimaki, T. Kawamata, T. Adachi, T. Noji, I. Watanabe, S. Ohira, W. Higemoto, and K. Nagamine, Int. J. Mod. Phys. B **14**, 3520 (2000).
- ⁹² C. Sire, C.M. Varma, A.E. Ruckenstein, and T. Giamarchi, Phys. Rev. Lett. **72**, 2478 (1994).
- ⁹³ D. Belitz and T.R. Kirkpatrick, cond-mat/0106279.
- ⁹⁴ H. Ding, J.R. Engelbrecht, Z. Wang, J.C. Campuzano, S.-C. Wang, H.-B. Yang, R. Rogan, T. Takahashi, K. Kad-owaki, and D.G. Hinks, cond-mat/0006143.
- ⁹⁵ I. Martin, G. Ortiz, A.V. Balatsky, and A.R. Bishop, Int. J. Mod. Phys. B **14**, 3567 (2000).
- ⁹⁶ C. Bernhard, J.L. Tallon, Th. Blasius, A. Golnik, and Ch. Niedermayer, Phys. Rev. Lett. **86**, 1614 (2001).
- ⁹⁷ J.L. Tallon, J.W. Loram, and G.V.M. Williams, cond-mat/0008295; however, note J. Bobroff, W.A. MacFarlane, H. Alloul, and P. Mendels, cond-mat/0008396.
- ⁹⁸ J.B. Goodenough and J.-S. Zhou, Phys. Rev. B **49**, 4251 (1994).
- ⁹⁹ H.H. Wen, W.L. Yang, and Z.X. Zhao, Physica C **341-8**, 1735 (2000), and H.H. Wen, X.H. Chen, W.L. Yang, and Z.X. Zhao, Phys. Rev. Lett. **85**, 2805 (2000).
- ¹⁰⁰ J.R. Cooper and J.W. Loram, J. Phys. I France **6** 2237 (1996).
- ¹⁰¹ R. Krupke and G. Deutscher, Phys. Rev. Lett. **83**, 4634 (1999); A. Sharoni, G. Koren, and O. Millo, cond-mat/0103581.
- ¹⁰² S. Rusiecki, E. Kaldis, E. Jilek, and C. Rossel, J. Less Comm. Metals **164**, 31 (1990).
- ¹⁰³ D. Allender, J. Bray, and J. Bardeen, Phys. Rev. B **7**, 1020 (1973).
- ¹⁰⁴ Y.J. Uemura, Physica C **341-8**, 2117 (2000).
- ¹⁰⁵ Y.J. Uemura, A. Keren, L.P. Le, G.M. Luke, W.D. Wu, Y. Kubo, T. Manako, Y. Shimakawa, M. Subramanian, J.L. Cobb, and J.T. Markert, Nature **364**, 605 (1993).
- ¹⁰⁶ R.S. Markiewicz and B.C. Giessen, Physica C **160**, 497 (1989).
- ¹⁰⁷ J. Corson, R. Mallozzi, J. Orenstein, J.N. Eckstein, and I.

- Bozovic, Nature **398**, 221 (1999).
- ¹⁰⁸ Z.A. Xu, N.P. Ong, Y. Wang, T. Kakeshita, and S. Uchida, Nature **406**, 486 (2000).
- ¹⁰⁹ C. Bernhard, D. Munzar, A. Golnik, C.T. Lin, A. Wittlin, J. Humlíček, and M. Cardona, Phys. Rev. **B61**, 618 (2000).
- ¹¹⁰ C. Meingast, V. Pasler, P. Nagel, A. Rykov, S. Tajima, and P. Olsson, Phys. Rev. Lett. **86**, 1606 (2001).
- ¹¹¹ G. Baskaran, Mod. Phys. Lett. **B14**, 377 (2000).
- ¹¹² B. Batlogg and V.J. Emery, Nature **382**, 20 (1996).
- ¹¹³ V. Barzykin and D. Pines, Phys. Rev. **B52**, 13585 (1995); J. Schmalian, D. Pines, and B. Stojkovic, Phys. Rev. Lett. **80**, 3839 (1998).
- ¹¹⁴ B. Batlogg, H.Y. Hwang, H. Takagi, R.J. Cava, H.L. Kao, and J. Kwo, Physica **C235-240**, 130 (1994); J.L. Tallon, J.R. Cooper, P.S.I.P.N. de Silva, G.V.M. Williams, and J.W. Loram, Phys. Rev. Lett. **75**, 4114 (1995).
- ¹¹⁵ M. Ido, N. Momono, and M. Oda, J. Low. T. Phys. **117**, 329 (1999).
- ¹¹⁶ V.J. Emery and S.A. Kivelson, Nature **374**, 6521 (1995).
- ¹¹⁷ R.S. Markiewicz, J. Phys. Cond. Matt. **2**, 665 (1990); A. Himeda and M. Ogata, Phys. Rev. Lett. **85**, 4345 (2000).